PROTON (HEAVY ION) RADIOGRAPHY IN MEDICAL DIAGNOSIS

V. W. Steward

Abstract

Beams of sub-atomic particles, particularly of protons and other heavy ions, may be used for safe, noninvasive diagnosis in medicine. These radiations supplement those of the electromagnetic spectrum and of sound. With their aid radiographs of unusually high contrast are obtained for the visualization and differentiation of the body tissues at very low doses. The method appears practical for use in hospitals and has potential for screening purposes. This report summarizes the basic aspects of the method and some results obtained by its use, with comments on its potential.

The Production of High Contrast Radiographs

Figures 1 and 2 illustrate, respectively, the fundamental differences in transmission and in depth-dose distribution between a beam of monoenergetic protons and a beam of x-rays in the diagnostic energy range, when both are passed through a homogeneous absorber (1,2). These differences are typical of heavy ions and of x-rays in general. It can be appreciated that a detector placed near the end-of-range of the protons will see a large change in intensity for a small change in effective absorber thickness. This difference in available contrast (shown in Figure 1) allows, for a given input, significantly more useful informational content in the downstream signal when using the particles. Moreover, advantage may be taken of the depth-dose distribution of the heavy ions to avoid a high first-surface dose, and to place the Bragg peak of ionization downstream of the region under examination. Thus, unlike with x-rays, a high first-surface dose can be avoided, such that the dose delivered throughout the depth of the absorber (tissue) is approximately uniform. By this means an image sensitive to slight changes in tissue density or hydrogen content is safely produced.

The degree of contrast within a heavy ion radiographic image depends on the slope of the range curve near the mean range of the particles (Figure 1). It
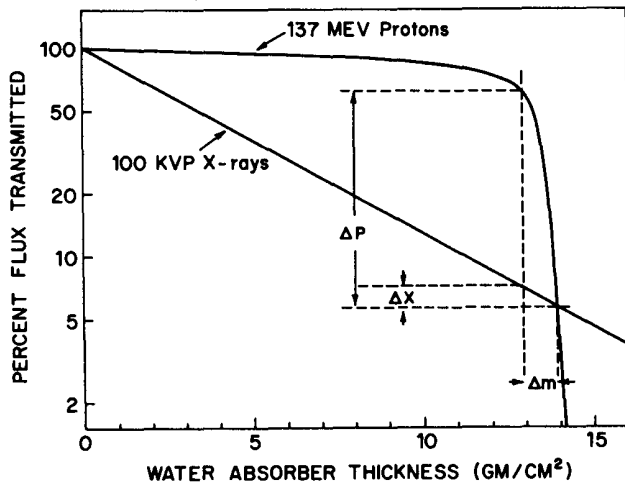

Figure 1. Flux-depth curves for protons and x-rays passing through a homogeneous medium. Note the difference in available contrast between the two rays for the detection of mass differences.

V. W. Steward
Department of Neurosurgery
University of Chicago
Chicago, Illinois

is thus influenced by the "straggling" of the particles about the mean range. In turn the "straggling" is influenced by the mass of the particles and by the energy spread of the beam. The heavier the particles and the more monoenergetic the beam the greater the contrast. The higher the contrast, however, the less the range of structural variations within an object which would appear in a single image plane. This range would equal the width of the end-of-range slope. Conversely, greater structural latitude may be obtained at the expense of lower contrast. In practice, a compromise is necessary according to the type of diagnostic information required.
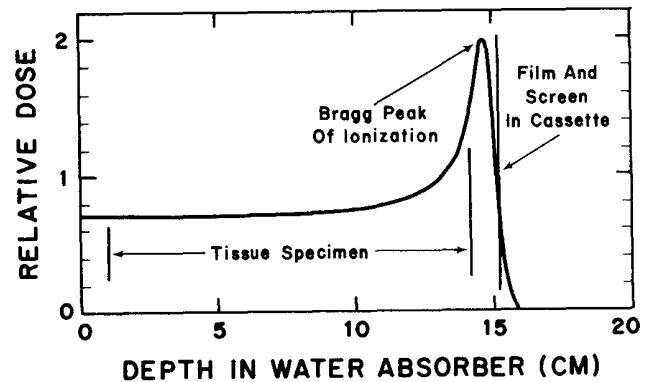
DEPTH-DOSE CURVE

Figure 2. Dose-depth curve for 148 MeV protons in water, showing the Bragg peak of ionization near the end of the particle range. The position of the region examined (tissue specimen) and of the screen-film detector relative to the Bragg peak are indicated.

Whereas the ionization interactions of the heavy ions are advantageous for radiography, the multiple Coulomb scattering they undergo can create a serious problem. By elastically deflecting the particles from their initial line of flight it causes crossovers to occur between adjacent regions. This leads to a decrease in both spatial resolution and in image contrast. Although the phenomenon is an important factor in end-of-range radiography, it can be minimized by matching the particle range to the object thickness and by placing the object as near as possible to the image plane. In fact, the mechanism has been used to advantage in producing radiographs analogous to those obtained by xero-radiography (3). Details concerning the transmission of heavy ions and the influence of absorber characteristics are given elsewhere (4).

Clearly, heavy ion radiographs can be made of an object by measuring the modulations in either the scattered or transmitted flux of the particles. Each technique differs in the type and level of information revealed, and in the radiation dose required. However, of all the techniques available, the end-of-range method appears to offer the greatest potential for medical diagnosis. This is because it provides the greatest contrast sensitivity at the lowest dose. Though radiography using multiple Coulomb scattering provides better spatial resolution (3), it is not so sensitive to density variations as the end-of-range method. Moreover, pathologic lesions in the human body rarely have clear-cut edges, or large differences in density with their surrounds by which advantage

may be taken of the mechanism. For this reason it would appear of restricted diagnostic value. Similarly, scatter radiography employing large angle scattering, though providing useful information on a given volume of absorber, would appear restricted by considerations of dose and expense of equipment (5).

The sensitivity of the end-of-range method may be gauged by noting that with film areal density differences of 0.05% have been routinely observed (6). This is to be compared with 0.22% obtained with x-radiographic film under exceptionally good conditions (7). With a split-beam scanning method, analogous to optical densitometry, an extremely high sensitivity of the order of 50 ppm has been obtained (8) and this could be improved to 20-30 ppm (9).

Some Experimental Results

The first images of human tissues using heavy ion radiography were obtained in 1971 on fixed autopsy material using the 160MeV proton beam from the Harvard cyclotron (1). In these, as in all subsequent work, the specimens were immersed in water contained within a plastic box with parallel faces; this minimized the effects of shape variation. Also, comparisons have been made throughout with optimum x-radiographs of the specimens, including precise correlations of the images with the pathologic findings.

Figure 3 demonstrates the type of result obtained. Earlier work had shown that in contradistinction to x-radiography human brain tumors, strokes, and the lesions of multiple sclerosis were well visualized when viewed outside the skull (1,2, 10). The images in Figure 3 suggest that in certain clinically simulated situations it will be possible to record directly a brain tumor within the skull. The result is also of interest since it was the first direct visualization on film of a noncalcified brain tumor (11). Similarly, a small (6 ml) simulated intercerebral haematoma has been directly visualized at a low dose in a fresh brain within a cadaver head (10).
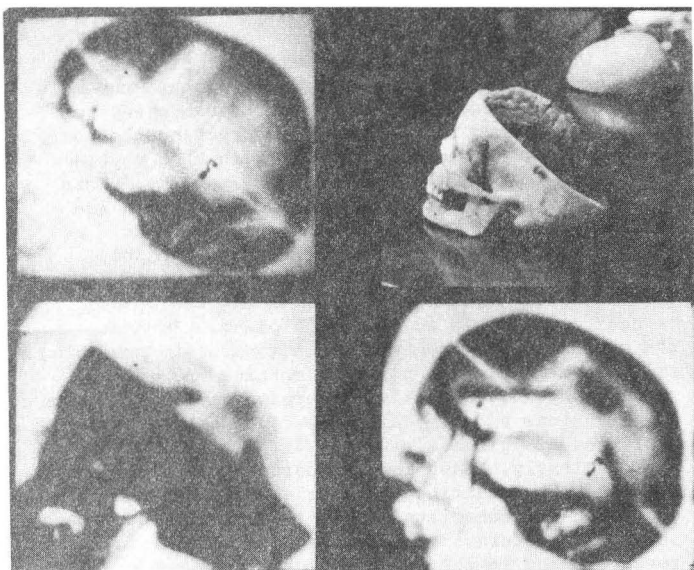

Figure 3.
(Upper left:) Proton radiograph (positive) of normal formalin-fixed human brain autopsy specimen placed within a skull in a water tank. Comparison with a similar picture taken with the brain removed (not shown) indicates some areas of increased density coming in from the periphery.
(Upper right:) Photograph of the right hemisphere of a human brain placed within the lower portion of a skull. Two strips of lead attached to the brain point towards a small portion of the tumor extending to the medial surface of the hemisphere.
(Lower left:) Proton radiograph (positive) of the tumor-bearing hemisphere held in the lower portion of the skull. Note the ends of the lead markers pointing to the lesion.
(Lower right:) Proton radiograph (positive) of the brain and tumor in the complete skull. With the skull cap in place, despite the modulation of density due to variable bone thickness, the tumor density can still be seen.
All radiographs taken with Radelin TF intensifying screen and Polaroid film. First surface dose less than 0.5 rad.

Other specimens which have been examined include human aortae where the plaques of atherosclerosis have been visualized, a sarcoma of the femur, liver specimens in which primary and metastatic carcinomas including a benign haemangioma have been seen, and a heart in which a pulmonary embolus was revealed. Also because of the importance of safely detecting "early" breast cancers several series of investigations have been devoted to examining fresh breast specimens, including a living patient (12,13).

The potential value of the method may be exemplified by the breast specimen results. Here, despite non-optimum taking conditions, the primary tumor and previously unsuspected small "satellite" cancers were revealed. One investigation on 17 fresh mastectomy specimens was performed with a 200 MeV proton beam where 100 MeV would have been more suitable, and used a back detector (film) in which scattering is a serious problem (13). Nevertheless, a total of 12 "satellite" cancers down to 3-4mm diameter were revealed. Importantly, these were seen with doses of 25-100 millirads, and had been completely missed by xeromammography at doses around 2.5 rads. Also, meticulous pathologic examination showed that no lesion had been missed, and that there was a one-to-one correspondence between the proton radiographic images and the structures within the specimens (13).

Overall, the work to date has borne out the theoretical prediction that the soft tissues should be visualized better by heavy ions than with x-rays. This is further supported by some interesting work on the computed tomographic scanning of physical test objects (14). Of equal importance, however, are the low radiation doses employed. Low doses have been alluded to above, but with a scanning procedure tumors have been revealed in a mastectomy specimen with a dose of approximately 3.7 mrad, and a haematoma in a fresh brain specimen with a dose of only 1.7 mrad. In fact, a recognizable image of a biological test object was obtained with an incident dose of about 1×10^{-4} rad, equivalent to the environmental radiation an individual experiences in 8 hours at sea level (15). To this must be added the results of studies which indicate that the relative biological effect of protons of the energy range required is equal to that of x-rays (RBE = 1.0) (16). These pieces of evidence speak to the safety of the method.

Nevertheless, despite the encouraging evidence which has been cited, more basic work was required in order to determine the clinical potential of the method. Of crucial importance was a proper understanding of what the human body presented to the ion beam in terms of density and stopping power. With regards to tissue density a search of the literature going back 216 years revealed this to be an inadequately studied subject from the radiographic point of view. Accordingly, an investigation was undertaken in which results were obtained on specimens from over 228 human cases (17). From this study it was concluded that the solid organs and their sub-divisions possess characteristic density differentials, and that
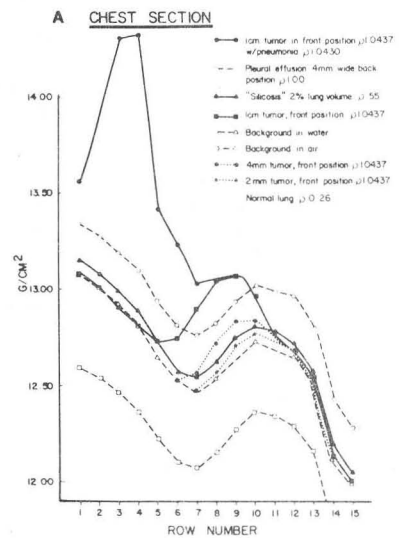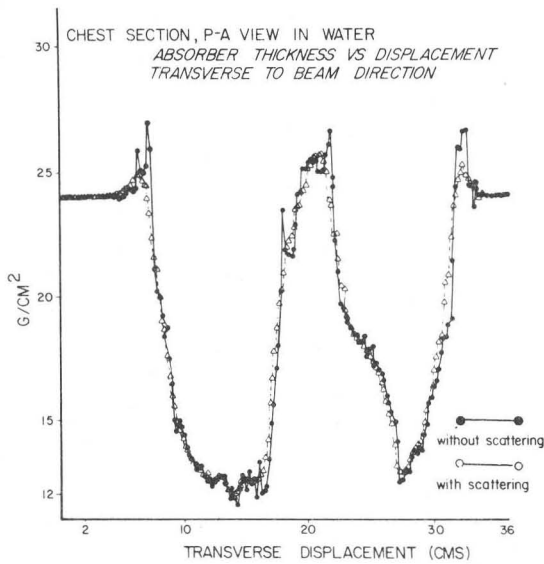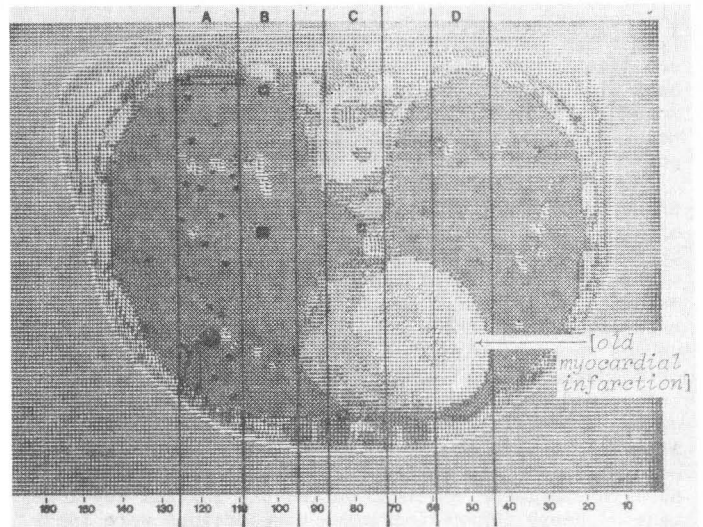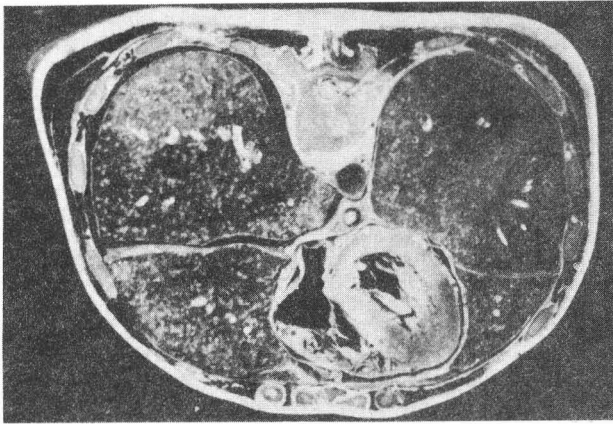
Figure 4.

(Upper left:) Photograph of section of human chest at level of 7th thoracic vertebra.

(Upper right:) Density array of section immersed in rectangular water box; matrix elements 2 mm². Four simulated 200 MeV proton beams (energy spread 1 MeV, FWHM), 25 rows across, with 600 protons/row traversed the section. Shown are the central 15 rows (A, B, C, and D, respectively), with density anomalies inserted, within which analyses were performed. Row A contains: at back, 4 mm deep pleural effusion; at front, 1 cm² cancer → 2 mm² ± associated wedge of pneumonia, and scattered nodules occupying 2% of lung volume, equivalent to 1 mm² nodules found in silicosis and "black lung" disease. Rows B and C contain 4 mm² tumors. Row D contains scar from old myocardial infarct (MI).

(Center left:) Comparison of direct integrated density pattern with pattern resulting from multiple scattering.

(Center right:) Differences in total absorber thickness due to density anomalies in Row A. In this and the other rows, all cases are above the critical value in the T² test.

(Lower right:) Same, due to old MI's of slightly different sizes in Row D (Δρ with heart muscle = 0.51%).
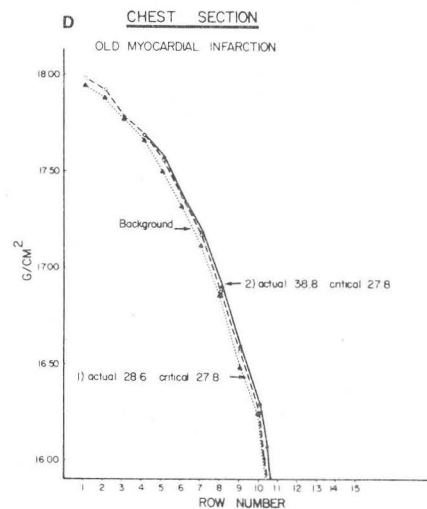
lesions such as cancers have densities which differ from their surroundings. These density differences are significant when considered in relation to the sensitivity of the heavy ion radiographic method. Moreover, they are in keeping with the results of a separate study in which the linear proton stopping power was measured directly on 100 tissue samples.

The next step was to use the density data in order to determine the range and relative variations of integrated densities one might expect when radiographing a human subject, and also to determine the sizes and densities of tissue anomalies which can be detected by protons near their end of range. For this calibrated photographs were taken of representative sections through a preserved human body. A grid system of 2mm^2 squares was then superimposed onto life-sized projections of the pictures. The density of the tissue falling within each grid square was assigned to that square. To simulate the sections being viewed while immersed in a water tank--a procedure that will be required during the initial development of heavy ion radiography--the sections were inscribed within rectangular matrices and unit densities assigned to all unoccupied squares. The cross sections in the form of density arrays were then loaded into a computer.

Before each computer run, the program reconstructed one of the stored density sections and placed it in a simulated proton beam in a manner analogous to that required for producing an actual radiograph. Each beam proton was followed by a Monte Carlo program as it traversed the section. The effects of multiple scattering and ionization energy losses on the proton trajectory were taken into account by the model. Nuclear scattering was ignored since protons undergoing these interactions do not contribute to the radiographic image. The dose delivered during image formation, however, was corrected to account for nuclear encounters. The proton transmission through the section as a function of position transverse to the beam direction was modulated according to the total amount of material traversed by the protons. This 1-dimensional proton transmission pattern was interpreted by the model as the radiographic image.

For detection of density anomalies two criteria were used. One criterion was that there be a 4% transmission difference significant to three standard deviations between the protons which passed through the anomaly and those which traversed the surrounding tissue. This transmission difference has been shown to be a reasonable lower limit. The second criterion was that an $\ell\Delta\rho$ of 0.05%, significant to the 5% level, be projected downstream by a density anomaly. An $\ell\Delta\rho$ of 0.05% had previously been shown detectable on film using a Berger phantom as a physical test object. The significance of discrimination between the two sets of data, i.e., background and background plus anomaly, was determined by the Hotelling T^2 test. Figure 4 illustrates the type of results obtained on a section through the chest.

It can be seen that, as expected, multiple scattering causes a smoothing over of the proton transmission pattern compared with the direct integrated density pattern, and that immersion in tissue-equivalent fluid, whilst reducing the total range variation in proton transmission, preserves the variations in range due to internal structural changes. This is useful with respect to reducing the dynamic range requirements on detector systems.

All the lesions illustrated, including many others in the head and abdomen, produced significant changes in proton transmission according to the Hotelling T^2 test. However, the test is but a statistical statement of the difference in signal-to-noise generated in each case, and was used as an arbitrary minimum in view of the great subjectivity of detection in real life situations. It gives no insight into the actual size, shape, density, or depth location of an anomaly, but only an estimate of the overall effect of these. Nevertheless, the results are encouraging in that many important lesions would appear to be detectable at low doses. This would be especially true with the summation of information and the avoidance of background available with computed tomographic methods.

The Diagnostic Potential of Heavy Ion Radiography

It is too early yet to specify how useful heavy ion radiography may be in medical diagnosis. However, there are a number of reasons which suggest that its value will be considerable.

First, the technique utilizes hitherto unexploited tissue characteristics, and in this sense may be said to open up a new "window" for probing the human body. Second, the greater available contrast compared with x-rays allows a significantly superior visualization of lesions within the soft tissues. Third, the detection of lesions by heavy ion radiography is considerably safer than by x-radiography. This suggests a great potential for screening purposes. Fourth, the interaction of heavy ions with matter is about as well known as that of x-rays and allows accurate predictions to be made. In addition to these, the human body presents a relatively enormous range of densities (from air SG = 0.0012 to bone SG = 1.8).

The value of the technique will depend on how it fits into the array of diagnostic methods available to the clinician. Nevertheless, as a noninvasive method with a wide margin of safety it promises much for early diagnosis. With respect to cancer, two-thirds of all cancer patients have metastases at the time the primary tumor is detected. Heavy ion radiography should help establish a diagnosis before spreading occurs. Thus 3-4 mm breast cancers have been detected at low doses where the probability of spread is negligible below 1 cm diameter. This should increase the 5-year survival for the disease from the 65th to the upper 90th percentile level, a not insignificant contribution considering 90,000 women per year contract the disease within the U.S.A. One hopes that similar benefits will accrue to lung cancer and heart attack patients. It should also take the detecting of intra-cranial lesions beyond that which is achievable with the latest x-ray scanners (now operating at very close to quantum detection efficiency), and lend precision to treatment planning for particle therapy.

Overall, the critical questions for heavy ion radiography are: (a) whether the potential described above can be proven in a true clinical setting; and (b) whether an economically feasible technology can be developed for the method's widespread use in hospitals.

It is hoped that a projected patient study program will provide much of the answer to the first question. With regard to the second the position also appears hopeful. Here it seems that nothing beyond the state-of-the-art in either accelerator or detector technology is required. In fact, a hospital-based proton synchrotron comparable in price with the whole body x-ray scanners has been proposed (18). Nevertheless, considerable thought is still required for the design of the most appropriate equipment.

In general, we have reason to believe that another powerful tool, as valuable as x-radiography is today, will be provided to the fight against disease. It is hoped that it will be perceived as an exciting and important challenge to those who build accelerators.

References

1. STEWARD, V. W., AND KOEHLER, A. M.: Proton beam radiography in tumor detection. Science 179, 913 (1973).

2. STEWARD, V. W., AND KOEHLER, A.M.: Proton radiographic detection of strokes. Nature, 245, 38 (1973).

3. WEST, D., AND SHERWOOD, A. C.: Radiography with 160 MeV Protons. Nature 239, 157 (1972).

4. BETHE, H. A., AND BLOCK: See for example "W. H. Barkas and Berger, M. J., in 'Studies in Penetration of Charged Particles in Matter.'" National Academy of Science Publication 113, p. 103 (1964).

5. SAUDINOS, J.; CHARPAK, G.; SAULI, F.; TOWNSEND, D.; AND VINCIARELLI, J.: Nuclear scattering aplied to radiography. Physics 20, 6, 890-905 (1975).

6. CURRY, J., AND STEWARD, V. W.: The Response of Screen Film to End-of-Range Proton Exposures. Nuclear Instruments and Methods 147, 541-5 (1977).

7. HALMSHAW, R., editor. Physics of Industrial Radiology, Chap. 9, 216-63, Heywood Books. London (1966).

8. KOEHLER, A. M., AND PRESTON, W. M.: A detector for small changes of areal density. Unpublished manuscript.

9. BELL, R. A., et al. A Nondestructive Measurement of the Fluctuations of Area Density of a Graphite Block using a 147MeV Proton Beam, Report AERE-R 5732, Atomic Energy Research Establishment, Harwell, England (1968).

10. STEWARD, V. W. Are X-rays the Ultimate? Proton (Heavy Ion) Radiography in Neurologic Diagnosis. J. Neurol. Sci. 39, 261-293, 1978.

11. STEWARD, V. W., AND KOEHLER, A. M.: Proton radiography of a human brain tumor within the skull. Surg. Neurol. 2, 283 (1974).

12. STEWARD, V. W., AND KOEHLER, A. M.: Proton radiography in diagnosis of breast carcinoma. Radiology 110, 217 (1974).

13. STEWARD, V. W., et al. The Proton (Heavy Ion) Radiographic Detection of Satellite Cancers and Other Lesions in Breast Specimens. To be published.

14. HANSON, K. M., et al. The Application of Protons to Computer Tomography IEEE Trans Nuclear Science Proc. Nuclear Sci Symp, Oct. 1977, San Francisco.

15. GOTTCHALK, E.; BOYD, D.; KOEHLER, A. M.: Private Communication.

16. ROBERTSON, J. B., et al. Radiobiological Studies of a High-Energy Modulated Proton Beam Utilizing Cultured Mammalian Cells, Cancer 35, 1664-77, (1975).

17. STEWARD, V. W.: The Density of Normal and Pathologic Human Tissues. To be published.

18. MARTIN, R. L.: An Accelerator for Proton Radiography Proceedings IV All-Union National Conference on Particle Accelerators 370-4, Moscow, USSR, Nov. 18-20 (1974).

** DISCUSSION **

K. ERDMAN: What do you consider the best proton energy to use for your work?

V. W. STEWARD: The best proton energy is that which allows the particle range to just exceed that presented by the region under examination plus about 2 g/cm^2 to place the Bragg peak downstream to the tissues. Thus the proton energy should range from about 100 MeV for examination of such structures as the breast, to 250 MeV for the head and pelvis.